Microtopographic Variation as a Potential Early Indicator of Ecosystem State Change and Vulnerability in Salt Marshes

Alexander Smith[1,2], Glenn Guntenspergen[3], Joel Carr[3], David Walters[3], Matthew Kirwan[1]

[1]Virginia Institute of Marine Science, William & Mary, Gloucester Point, VA, 23062, USA
[2]Smithsonian Environmental Research Center, Edgewater, MD
[3]U.S. Geological Survey, Eastern Ecological Science Center, Laurel, MD, 20708, USA

Abstract: As global climate change alters the magnitude and rates of environmental stressors, predicting the extent of ecosystem degradation driven by these rapidly changing conditions becomes increasingly urgent. At the landscape scale, disturbances and stressors can increase spatial variability and heterogeneity – indicators that can serve as potential early warnings of declining ecosystem resilience. Increased spatial variability in salt marshes at the landscape scale has been used to quantify the propagation of ponding in salt marsh interiors, but ponding at the landscape scale follows a state change rather than predicts it. Here, we suggest a novel application of commonly collected Surface Elevation Table (SET) data and explore millimeter-scale marsh surface microtopography as a potential early indicator of ecosystem transition. We find an increase in spatial variability using multiple metrics of microtopographic heterogeneity in vulnerable salt marsh communities across the North American Atlantic seaboard. Increasing microtopographic heterogeneity in vulnerable salt marshes mirrored increasing trends in variance when a tipping point is approached in other alternative stable state systems – indicating that early warning signals of marsh drowning, and ecosystem transition are observable at small-spatial scales prior to runaway ecosystem degradation. Congruence between traditional and novel metrics of marsh vulnerability suggest that microtopographic metrics can be used to identify hidden vulnerability before widespread marsh degradation. This novel analysis can be easily

applied to existing SET records expanding the traditional focus on vertical change to additionally encapsulate lateral processes.

Keywords: wetland vulnerability, microtopography, ecosystem state change, sea-level rise

Acknowledgements: Primary funding for this work comes from the USGS Ecosystem Mission Area and Climate Research and Development Programs with additional support from the National Science Foundation (#1654374, #1832221, and #2012670). Any use of trade, firm, or product names is for descriptive purposes only and does not imply endorsement by the US Government.

Introduction

Salt marshes provide critical ecosystem services, but are threatened by sea-level rise and diminishing sediment availability that together lead to erosion and marsh submergence (Hopkinson *et al.*, 2012; Temmerman *et al.*, 2013; Kirwan and Megonigal, 2013). Regional and global assessments predict that sea-level rise (SLR) alone could lead to the loss of 20-50% of marshes by the end of the century (Craft *et al.*, 2009; Kirwan *et al.,* 2016). On the other hand, feedbacks between vegetation, inundation, and sediment transport allow some marshes to persist with SLR as stable ecosystems for millennia (Kirwan and Megonigal, 2013). Predicting the fate of tidal marshes to SLR is hotly debated (Kirwan *et al.*, 2016; Schuerch *et al.*, 2018; Tornqvist *et al.*, 2021; Saintilan *et al.*, 2022), driven in part by the realization that early warning signals are difficult to detect in systems with non-linear or “catastrophic” transitions (Wilson and Agnew 1992; Scheffer *et al.*, 2001).

The collapse of salt marshes is often expressed through the runaway growth of unvegetated ponds that consist of shallow depressions filled with standing water and occur within the marsh interior (Mariotti, 2016). The transition between stable, vegetated marsh and unvegetated pond is abrupt, commonly irreversible, and driven by positive feedbacks that separate them into two alternative states (Wang and Temmerman, 2013) Once ponds form, positive biophysical and biochemical feedbacks expand the ponded area, which potentially leads to permanent marsh loss (Stevenson *et al.,* 1985; DeLaune *et al.*, 1994; Mariotti and Fagherazzi, 2013; Mariotti, 2016; Himmelstein et al., 2021). As ponds proliferate in the marsh landscape, extensive pond networks decrease wetland stability through enhanced sediment export and reduced sediment trapping (Stevenson *et al.*, 1985; Ganju *et al.*, 2013; Ganju et at al., 2017).

Salt marsh vulnerability assessments often rely on comparisons between the rate of SLR and point-based measurements of marsh elevation change or vertical accretion rates (Reed 1995; Raposa *et al.,* 2016). While these traditional methods capture vertical stability, they underestimate spatio-temporal variability and neglect lateral processes, such as ponding, erosion, and lateral migration, across the landscape (Kirwan *et al.,* 2016; Ganju *et al.,* 2017). Recent modelling indicates that these neglected lateral dynamics are especially important as biophysical feedbacks maintain marsh stability in the vertical direction but not the lateral direction (Mariotti and Fagherazzi, 2013; Mariotti and Carr, 2014). Therefore, these traditional metrics of wetland vulnerability neglect spatial dynamics that may be more representative of whole-ecosystem resilience and offer clues to impending ecosystem transitions.

The Surface Elevation Table (SET) method is a global standard for assessing wetland vulnerability to SLR through the monitoring of vertical elevation change (Cahoon *et al.*, 2006; Webb *et al.*, 2013; Raposa *et al.*, 2016; Jankowski *et al.*, 2017; Saintilan *et al.*, 2022). The method measures elevation change relative to a stable benchmark and is typically paired with an artificial marker horizon (consisting of feldspar, clay, or sand) to capture the suite of biophysical processes contributing to the gain (e.g. accretion, root expansion, soil dilation) and loss (e.g. subsidence, erosion, compaction) of marsh elevation change through time (Callaway *et al.,* 2013). SET stations are used extensively; from 1997 to 2017 at least 985 SETs were installed within the state of Louisiana, U.S. (Covington, 2020) and over 1,000 SET stations on the mid-Atlantic U.S. coast were affected by Hurricane Sandy in 2012 (Yeates *et al.,* 2020).

SET stations have been utilized in numerous field studies (Baustian *et al.,* 2012; Lovelock *et al.*, 2015; Blum *et al.*, 2021), coordinated wetland monitoring networks (Raposa *et al.,* 2016; Jankowski *et al.,* 2017), and global reviews to quantify wetland vulnerability (Saintilan *et al.,* 2022). However, the collected data are underutilized by focusing on solely the vertical component. Because SET stations measure elevation at multiple discrete points within the same local area through time, these stations additionally capture changes in the microtopography of the marsh surface, though this metric is seldom employed or even analyzed (Smith *et al.,* 2022). While the focus on the vertical component of SET records follows traditional understandings of marsh vulnerability to SLR, analyzing changes to the variation within SET records may aid in detecting early warning signals of wetland degradation prior to ecosystem state change.

Microtopography, the small scale variation in ground surface height (centimeter to millimeter scale) over short spatial scales (meter scale), in wetland ecosystems is driven by numerous abiotic and biotic drivers as well as the interactions between them (Fig. 1a; Diamond *et al.*, 2021). While these numerous drivers create a spatially complex surface microtopography, climate change imparts directional changes on these drivers to have cascading changes to microtopography (Fig. 1a). Similar dynamics can be seen at the landscape scale, where accelerating rates of SLR are homogenizing not just the landscape diversity of marshes, but also the topography (Mariotti *et al.,* 2020; Schepers *et al.,* 2020). As ponds dominate the landscape, average elevation of the landscape falls because ponds exist as a stable alternative state at lower elevations (Watson *et al.,* 2017; Schepers *et al.,* 2020). However, the distribution of landscape-averaged elevation is non-stationary as the elevation variance of the landscape initially increases during the transition period between alternative stable states (Schepers *et al.,* 2020; Wang *et al.,* 2021). We hypothesized that wetland microtopographic variation will similarly increase in these highly vulnerable ecosystems (Fig. 1b). Uniquely, while this variance is likely to follow the same pattern during the "catastrophic", non-linear transition between alternative states (Wilson and Agnew, 1992; Scheffer *et al.,* 2001), increasing microtopographic variation may serve as an early warning signal of ecosystem state change.

To examine whether microtopography can be used as a novel indicator of vulnerability and to explore if microtopographic variation could be an early indicator of ecosystem state change in salt marshes, we analyzed changes in four metrics of microtopographic variation across ~14 years of SET data from 20 SET stations across the U.S. mid-Atlantic coast and Northeast. Here, we show that these four metrics of changing microtopographic variation correlate with traditional metrics of wetland vulnerability and that these microtopographic metrics may be an early warning indicator of state change in wetlands that are likely to be vulnerable to future rates of SLR.

Methods

Approach

Eight tidal salt marshes along the Atlantic Coast of the United States, ranging across Virginia at the southern extent and Maine at the northern extent, were selected for study. Specifically, we examined salt marshes within Saxis Wildlife Management Area (SX) in

Virginia, Fishing Bay Wildlife Management Area (FB8), Blackwater National Wildlife Refuge (BW7), the Smithsonian Environmental Research Center at Hogs Island (HI), and Eastern Neck National Wildlife Refuge (EN) in Maryland, Bombay Hook National Wildlife Refuge (BH) in Delaware, Great Meadows National Wildlife Refuge (GM) in Connecticut, and Rachel Carson National Wildlife Refuge (RC) in Maine (Fig. 2). Within this extent the 50-year averaged rates of SLR ranged from 4.00 mm y^{-1} in Virginia (SX), where rates were twice as high as eustatic rates (~ 2 mm y^{-1}), to 1.90 mm y^{-1} in Maine (RC) (Table 1). Porewater salinity at these sites ranged between 8.9-19.9 ppt (Guntenspergen et al., 2023; Table 1). The unvegetated to vegetated ratio (UVVR) of marsh vegetation within these sites, specifically the 100 m^2 area surrounding the SET stations, ranged from 0.94, which indicates nearly complete unvegetated marsh, to 0.001, indicating near ubiquitous vegetated marsh (Saintilan et al., 2022; Table 1).

At each of these reserves, two surface elevation stations (SETs) were installed within salt marshes to monitor elevation changes driven by SLR with the exception of FB8 and BW7 where four SETs each were installed, which are distinguished through the addition of A or D after the site identification labels (Table 1). SET stations are comprised of a deep rod SET marker that is installed deep into wetland soils until reaching refusal to which a receiver is attached. The SET arm can be affixed to the receiver and then rotated to four of eight permanent positions on the receiver. The SET is a portable device that provides repeatable, high-precision measurements of relative elevation change at consistent locations within coastal wetlands. This portable instrument extends horizontally over the marsh surface and from this extended arm, eight pins at fixed points along the instrument are lowered to the marsh soil surface and the heights of those pins above the arm are measured. At the next measurement event, these pins reoccupy the same location on the wetland surface and are measured again. This repetitive measurement monitored through time examines changes to marsh surface elevation. Pin lengths are not measured if the marsh surface is obstructed, such as by wrack deposits or ice deposits. The footprint of an SET is approximately 0.7 m^2 with pin lengths measured over four ~30 cm subsections of the footprint. See Lynch *et al.*, (2015) for extended details about SET instrumentation.

Most SET stations were installed in 2005 with the first measurement taken between July to September of 2005, except for SX, GM, and RC, which were installed in 2006 and were first sampled in March and May of 2006. The eight marshes that we analyzed in this study were established by the U.S. Geology Survey in 2005, to develop a geographically broad network of coastal elevation monitoring stations with standard monitoring protocols to determine how coastal wetland surface elevations trends respond to sea-level rise and nutrient addition. Because of the long-term nature of the study, sites were established in federal, or state protected preserves which included national wildlife refuges (EN, BW, BH, GM, and RC), state wildlife management areas (FB, SX), and the Smithsonian Environmental Research Center (HI). Only the control plots at each site were chosen for this study. All SETs were monitored with the same frequency for at least 13.5 years with collection dates occurring within 1-2 months of each other across the sites. SETs were measured at least twice yearly until 2008 after which SETs were measured once per year until 2019. SET stations were mostly installed above the site specific mean high water, except for the two SETs at BW7 which were 0.28 to 0.11 m below mean high water and, as sites, had limited land above mean high water. When installed, the dominant vegetation at most sites was either *Spartina patens*, *Distichlis spicata*, or *Schoenoplectus americanus* except for at RC where one SET was located within *Glaux maritima*. Vegetation density and changes to both density and species were not recorded through time.

Traditional Vulnerability Metric: Elevation Change Deficit

Elevation change was calculated by averaging the rate of elevation change for each pin (n=28-32) within a SET through time. Cumulative elevation trends were regressed at the pin level to increase precision and to consider serial autocorrelation. This method results in approximately 30 estimates of linear trends that were then averaged to the entire station to get one, average rate of elevation change. Comparison of surface elevation change rates to the rate of local SLR allowed for the calculation of the elevation change deficit (Cahoon *et al.,* 1995). Since the 1990s, elevation change deficits have been the benchmark for determining submergence potentials of wetland ecosystems (Cahoon *et al.,* 1995; Cahoon *et al.,* 2006; Cahoon, 2015; Lovelock *et al.*, 2015; Saintilan *et al.*, 2022; Steinmuller *et al.*, 2022). The general equation for elevation change deficit is:

$$E_{def}=E_c-SLR$$

Where E_c is the rate of elevation change (mm y^{-1}) and *SLR* is the local rate of SLR (SI Table 1). We utilized the 50-year averaged rate of SLR (mm y^{-1}) because it was found to be the greatest predictor of vertical accretion (Saintilan *et al.*, 2022). Rates of SLR were derived from the nearest National Oceanic and Atmospheric Administration (NOAA) tidal gauge with at least a 50-year record of sea-level. Typically, a marsh is considered vulnerable if the elevation change deficit is negative, which indicates that the measured elevation change rate is less than the selected rate of SLR. However, it should be noted that the time period over which rates of SLR are calculated can change vulnerability interpretation (Saintilan *et al.,* 2022). For example, elevation deficits calculated with SLR rates averaged over recent, shorter durations are typically more negative (i.e. indicating higher wetland vulnerability) because eustatic SLR rates are generally accelerating.

Novel SET-derived Microtopographic Vulnerability Metrics

Field measurements of microtopography consisted of pin length measurements taken along the SET arm. Our SET arm consisted of eight fixed points approximately 4 cm apart from which pins were lowered to the sediment surface and length was measured. The SET arm was rotated 90 degrees around the anchored center of the SET station and pin length was measured along the arm following each rotation resulting in approximately 32 measures of relative elevation (Fig. 3). Microtopography was quantified using four index measures: random roughness (RR), tortuosity (T), elevation range (ΔH), and the surface area to map area ratio (SA:MA). Random roughness is the standard deviation of all pin readings at a point in time ($\sqrt{\frac{\sum(x_i - x_\mu)}{n-1}}$) and is the most suitable indicator of water storage in local depressions (Kamphorst *et al.,* 2000; Karstens *et al.,* 2016). Generally, random roughness describes the uniformity of the elevation distribution. For the two-dimensional path along each arm, the ratio of the over-surface distance to the corresponding straight-line path is referred to as tortuosity (Moser *et al.,* 2007; Karstens *et al.,* 2016; Smith *et al.,* 2022) and is defined as

$$\sum\sqrt{((x_2 - x_1)^2 + (y_2 - y_1)^2 + (z_2 - z_1)^2))/l)}$$

Where $(x_2 - x_1)$ and $(y_2 - y_1)$ are the respective distance in the x and y direction between adjacent pins, $(z_2 - z_1)$ is the difference in measured pin length, and *l* is the straight-line path length along the SET arm. This equation produces four tortuosity measurements per SET, one measure of tortuosity along each arm replication, which were then averaged to the plot level. The elevation range (ΔH) was calculated from the difference between the highest and lowest point measured at the SET during a sampling period and represents the magnitude of difference between extremes. SA:MA was calculated in a programming platform (Matlab version R2018b by first using the *griddata* function). This function fits a surface to scattered elevation data by interpolating a surface so that it passes through the data points and interpolates intermediate values according to a triangulation-based natural neighbor interpolation. The interpolated surface consists of a square surface encompassing the extent of the area that the SET arm covers with 32 interpolated values along each edge of the square for a total of 1024 interpolated points fitted to the 32 loaded data points (Fig. 3). The surface area of the interpolated surface was then measured (in Matlab using the *delauney* function), which created a 3-D Delauney triangulation from the points within the interpolated surface and returned the indices of the triangles. Using these indices, we then calculated the area of the individual triangles and the cumulative area of the interpolated surface. Finally, dividing the surface area of the interpolated surface to the footprint of the SET produced SA:MA. Tortuosity and SA:MA are both unitless ratios.

Microtopography of the marsh surface is likely to be variable between sites based off of local biotic and abiotic factors (Diamond *et al.,* 2021). For example, crab herbivory has been shown to create concave-convex surface formation while vegetation in hummock-hollow formations can preferentially trap sediment and increase surface elevation (Stirbling *et al.,* 2007; Qiu *et al.,* 2019). Therefore, to relate microtopography to vulnerability, we focused on the change in microtopography (SI Fig. 1). According to our hypothesis, we expected microtopographic variation to increase as a vulnerable system becomes more degraded (Fig. 1). Therefore to examine this hypothesis, we stipulated that these microtopographic metrics indicate vulnerability if the linear change in microtopographic variation increased significantly during the study period. Across all of these microtopographic metrics, increasing rates of change represent a marsh surface that is generally increasing in roughness. We then compared vulnerability as indicated by these microtopographic metrics to the elevation change deficit to examine the utility of these novel microtopographic metrics as vulnerability indicators. Linear regressions were fitted in Matlab and significance was tested using an F-statistic which tests the significance between two datasets – here the modeled linear relationship and a population showing a null hypothesis (i.e. stable microtopographic variation). Metrics that show significant changes in microtopographic variability were then cataloged in the Marsh Vulnerability Report Card (Table 2).

Results

Traditional Vulnerability Metric: Elevation Change Deficit

Elevation change data from the 20 SET stations indicated that rates of elevation change ranged from -7.8 to 5.9 mm y^{-1} over the duration of the records. Negative rates of elevation change, or elevation loss, were recorded at only two SETs, FB8D4 and BW7D4 (-7.8 and -0.9 mm y^{-1}, respectively). All other elevation change rates were greater than zero, indicating increasing surface elevation during the study period. Of these SETs, the average elevation change rate was 3.4 mm y^{-1} (± 1.2 mm y^{-1}, standard deviation) and was greatest at BH2 (5.9 mm y^{-1}) (SI Table 1). The elevation change deficit, the difference between elevation change and the 50-year averaged rate of local SLR (SI Table 1), ranged from -11.7 m y^{-1} (FB8D4) to 2.2 mm y^{-1} (BH2) (Fig. 4). Of the 20 SETs, seven had elevation change deficits significantly less than zero (with an average and standard deviation of -3.9 ± 2.0 mm y^{-1}), seven SETs displayed elevation change deficits not significantly different than zero (-0.5 ± 0.6 mm y^{-1}), and six SETs had significant positive elevation change deficits (1.5 ± 0.5 mm y^{-1}) (Fig. 4). Based on these elevation change deficits, we then classify our set of SETs into three categories: "vulnerable", where elevation change deficit is negative, "steady", where the elevation change deficit is not significantly different than zero, and "surplus" where the elevation change deficit is significantly positive (Fig. 5).

Novel SET-derived Microtopographic Vulnerability Metrics

Initial measurements of microtopography during the first sampling period indicated significant differences between SETs. For example, RR was highest at BW7D (1.2 mm), approximately 2.5 times rougher than the site with the lowest RR (SX4, 0.5 mm). However, an insignificant relationship was found between initial variability and change in microtopographic variation across all metrics (linear regressions; RR: R2=0.07, *p*-value =.25; T: R2=0.01, *p*-value=.62; ΔH: R2=0.03, *p*-value=.41; SA:MA: R2=0.04, *p*-value=.37). Sites where microtopographic variability increased significantly were categorized as vulnerable. RR increased at a rate significantly greater than zero across 12 SETs and consequently was the microtopographic metric that identified the greatest number of sites as vulnerable (Fig. 5a; Table 2). Tortuosity increased at a significant rate at eight SETs, all of which were also indicated as vulnerable by RR (Fig. 5b; Table 2). At 11 SETs, ΔH increased at a significant rate. However, two of these SETs (HI2 and HI3) were not indicated as vulnerable according to either the tortuosity or RR metrics (Fig. 5c; Table 2). Finally, SA:MA increased at a significant rate at six SETs (Fig. 3; Fig. 5d; Table 2). These SETs were indicated as vulnerable by all aforementioned microtopographic variation metrics. Across all of these microtopographic metrics, positive rates of change are associated with a marsh surface that is increasing in roughness generally (SI Fig. 1).

Discussion

Comparing Microtopographic Vulnerability and Traditional Vulnerability Metrics

Traditional analyses of wetland vulnerability utilizing SET data emphasize elevation change deficits, the difference between the rates of elevation change and local SLR, as a primary indicator of wetland vulnerability (van Wijnen and Bakker, 2001; Cahoon *et al.*, 2006; Kirwan and Temmerman, 2009; Cahoon and Guntenspergen, 2010; Cahoon, 2015). According to this traditional metric, seven of the SETs in this study are highly vulnerable to SLR while the other SETs are keeping pace with SLR (seven SETs) or increasing in elevation faster than the rate of SLR (six SETs) (Fig. 4, Fig. 5, SI Table 1). The collated novel metrics of changing microtopographic variation examined indicated similar results: six of the SETs indicate potential vulnerability according to all four metrics, eight were categorized as potentially vulnerable by one, two, or three metrics, and six were identified as potentially stable ecosystems (Table 2). While a limited sample size prevents the application of significant statistical regressions between the novel and traditional vulnerability metrics, six out of the seven SETs indicated by traditional metrics as highly vulnerable were positively identified as vulnerable by all novel microtopographic metrics (Fig. 6). This result suggests that microtopographic variation can be used to assess vulnerability in those wetlands that are at high risk of drowning from SLR. Of the SETs where the elevation change was approximately equal to the 50-year averaged rate of SLR, five out of the seven SETs were indicated as vulnerable by at least one microtopographic metric (Fig. 5, Fig. 6). This result could indicate that while these sites are keeping up with historic rates of SLR, modern rates may be exceeding marsh stability and increasing ecosystem degradation or an independent driver not captured in our dataset may be affecting microtopography, such as shifts in vegetation or herbivory (Fig. 1). Of the six sites with positive elevation change deficits and not considered vulnerable to SLR, two SETs were categorized as vulnerable by at least one microtopographic metric (Fig. 6). Without additional information regarding biomass density or vegetation shifts, it is impossible to determine if these indicators are false positives or indicators of a hidden vulnerability not captured in the elevation change deficit. For example, because microtopography is greatly affected by vegetation morphology and density, changing microtopography could be driven by SLR induced recovery time reductions or by independent changes in plant community (Bertness *et al.,* 1992; Diamond *et al.*, 2021). Additionally, abiotic drivers like wrack deposition and sediment accumulation can both increase variance or homogenize the marsh surface (Werner and Zedler, 2002). The limitations of this dataset prevent the examination of these co-occurring drivers, but the general congruence between microtopographic and elevation deficit relative to sea-level rise indicates that microtopographic changes can be used as a proxy for wetland vulnerability. A holistic model that integrates both traditional and novel microtopographic metrics as well as information regarding changes in vegetation density and species that affect both metrics may best encapsulate wetland vulnerability. Additionally, examining these changes in SET records that span the entire transition from the vegetated to ponded ecosystem states would better reveal how early microtopography can detect decreased vulnerability and therefore further resolve some of these potential false positives.

While the temporal and statistical limitations of this dataset prevent the definitive identification of changing microtopographic variation as an early indicator of imminent state change, we argue that the utility of microtopographic variation extends beyond traditional vulnerability metrics. For example, marshes in Plum Island Estuary, Massachusetts (42.717, -70.826) have low sediment budgets, limited area for landward migration, and negative elevation change deficits – all of which indicate high vulnerability to accelerating SLR (Farron et al., 2020; Langston et al., 2020). However, despite this perceived vulnerability, ponding in Plum Island marshes has been historically stable (Wilson et al., 2014) and marsh extent is forecasted to be largely maintained through 2100 (Langston *et al.,* 2021; Farron et al., 2020). Eventually, as the elevation change deficit reduces the elevation capital and lowers the marsh surface within the tidal frame, ponding will likely propagate throughout the landscape (Duran Vinent et al., 2021; Himmelstein et al., 2021), but elevation change deficit cannot predict these sudden changes as it already classified the marsh as vulnerable far prior to a critical ponding threshold (Langston *et al.,* 2021). Microtopography, specifically rapid increases in microtopographic variation, could be a more useful early indicator of this sudden state change, which is critical for rapid management actions in preserving these valuable, yet vulnerable ecosystems (Neijnens et al., 2021). Therefore, integrating these traditional metrics with these novel microtopographic metrics could bridge vulnerability assessments examining slow gradual drowning with fine-scale analyses predicting sudden state change.

Temporal and Spatial Scaling of Microtopography

Microtopography is driven directly by abiotic and biotic drivers that are influenced by climate forcing (Diamond *et al.*, 2021). Because of this cascading relationship, changes in microtopographic variation may be more sensitive to alterations to the climate than metrics like average vertical elevation change, which can be affected by events, such as storms and fires, but is a factor of dynamic biophysical feedbacks that operate at the decadal scale (Törnqvist *et al.*, 2021). Low-magnitude early indicators of abrupt ecosystem state changes may be homogenized in the decadal sediment record (Fagherazzi *et al.*, 2012). In contrast to this method, high resolution microtopography responds directly to biotic and abiotic changes that portend ecosystem state change, such as slower plant recovery or decreased belowground biomass, and may be valid as an early indicator of ecosystem degradation (Stribling *et al.*, 2007; van Belzen *et al.*, 2017; Diamond *et al.*, 2021). However, the high sensitivity of microtopography to these factors creates noise even under stable conditions (Stribling *et al.*, 2007; Harman *et al.*, 2014).

Therefore, similar to elevation trends measured using SETs, equilibration time is likely required to assess the magnitude of background fluctuations associated with a naturally variable living marsh surface (Lynch *et al.*, 2015; Blum *et al.*, 2021). While measuring microtopography over decadal periods can reveal general trends, limiting microtopographic variation to annual measurements may overemphasize temporary changes and homogenize short-term microtopographic cycles and negative feedbacks (Smith *et al.*, 2022). Ultimately, the extended application of these microtopographic vulnerability metrics described herein to regional and global SET datasets could potentially strengthen the possibility of microtopography as an early indicator of state change.

Elevation change deficits calculated at SET stations have been scaled-up to represent vulnerability of entire ecosystems and regions (Cahoon *et al.*, 2002; Wasson *et al.*, 2019). The spatial dependent nature of microtopographic measurements prevents similar direct scaling, but spatial heterogeneity can be measured at the landscape scale using LIDAR based digital elevation models (or DEMs) (Doughty *et al.*, 2021). For the past 20 years, many studies have used LIDAR to remotely sense ground elevation over large areas, but salt marsh vegetation structure and instrument error make it difficult to detect meaningful differences in elevation across the landscape at the microtopographic scale (Hladik and Alber, 2012). While recent advances in error correction can reduce error – for example reducing mean error from 0.16 m to 0.004 m (McClure *et al.*, 2015) – centimeter-scale horizontal resolutions homogenize across the millimeter-scale topography of the marsh surface that SETs quantify. At intermediate spatial scales (1-10 m) various methodologies exist to quantify topography, but coarse vertical resolution (chain length, drone imagery, real-time kinematic global positioning system (RTK-GPS) units), salt marsh vegetation (Terrestrial Laser Scanning), and a lack of long-term datasets currently limits the comparison between this intermediate spatial resolution and the sub-centimeter variance of the marsh surface.

The ratio of unvegetated to vegetated marsh (UVVR) has been suggested as an indicator of marsh health where wetland complexes are stable below UVVR values of 0.10 to 0.15 (Wasson *et al.*, 2019; Ganju *et al.*, 2022). UVVR is quantified independently of SLR, similar to microtopographic variation (Ganju *et al.*, 2017). However, the sensing of UVVR at the landscape scale necessitates imagery with a coarse horizontal resolution (from 3-30 m), which neglects ponds below this detection threshold (Ganju *et al.*, 2022). While the presence of larger ponds does have implications about ecosystem-scale functions and vulnerability, the formation of large ponds follows rather than precedes ecosystem state change (Duran Vinent *et al.*, 2021). Because of this temporal difference, there is a lack of correlation between UVVR and the novel microtopographic vulnerability metrics (SI Fig. 2). However, as the spatial and temporal resolution of UVVR datasets improves and we assess the spatiotemporal UVVR dynamics, comparisons of changing landscape heterogeneity with changing microtopographic variability may support insights into the spatial scaling of microtopographic vulnerability metrics.

Microtopographic Change as a Potential Early Indicator of Ecosystem Vulnerability

"Critical slowing down" is an early warning signal for impending state changes where the time required for a system to recover from a disturbance lengthens as the magnitude of stressor applied increases and typically results in an increase in spatial heterogeneity and stochasticity under applied stress (van Nes and Scheffer, 2007; Dakos *et al.*, 2008; van Belzen *et al.*, 2017). In coastal wetlands, vegetation recovery to disturbance slows with increasing inundation, thereby increasing the risk of marsh degradation (van Belzen *et al.,* 2017). Ponds and stable wetlands display a markedly bimodal elevation distribution with a low proportion of transitional, intermediary states within the marsh landscape and with little potential for unvegetated ponds to become revegetated (Wang and Temmerman, 2013; Watson *et al.*, 2017; Schepers *et al.*, 2020). Given the feedbacks that maintain ponds and marshes at their respective stable equilibria, ponds and wetlands have been proposed to reflect alternative ecosystem states, where early warning signals are critical for forecasting impending state changes prior to landscape-scale changes.

While landscape heterogeneity can encapsulate the degree of ecosystem degradation, changes in microtopographic variation potentially precede state change because microtopography is highly sensitive to the abiotic and biotic drivers that experience critical slowing down (van Belzen *et al.*, 2017; Diamond *et al.*, 2021). In wetlands, as vegetation recovery rates decrease with increased inundation stress from rising sea-levels, a greater proportion of the marsh platform is likely in or near a lower elevation degraded state following disturbances (van Belzen *et al.*, 2017; Schepers *et al.*, 2020). Therefore, microtopographic variation is expected to increase with inundation, making microtopography a potential leading indicator of landscape-scale ecosystem state change. While similar fundamental biophysical interactions between vegetation and morphology have been used to examine mechanisms that stabilize marsh resilience to SLR (Kirwan and Megonigal, 2013), this study presents the novel idea that changes in sub-meter scale topography can be used as an early indicator of looming state change that can be detected prior to large scale state changes that would be captured with traditional approaches to assessing wetland vulnerability.

Applying Microtopographic Vulnerability Metrics

While this study only reviewed SET records from 8 salt marshes along the U.S. mid-Atlantic and Northeast coasts, the novel metrics described can be easily applied to existing SET data records without requiring additional data collection or leveraged external variables, such as SLR. Because traditional metrics rely on rates of SLR, the time frame over which SLR is calculated can greatly change the perceived vulnerability of wetlands (Saintilan *et al.*, 2022). Microtopography data collected from SETs can be analyzed within the context of previous wetland conditions thereby making vulnerability relative to historical conditions of the marsh surface rather than to external drivers. Additionally, while this study only examined salt marshes, SETs are widely used in a number of coastal ecosystems, such as mangrove forests (Lovelock *et al.*, 2015), tidal freshwater forests (Krauss et al., *in review*), and mud flats (Marion *et al.*, 2009), to quantify ecosystem vulnerability and could be implemented in peatlands where microtopographic formations arise from climate induced feedbacks (Harris *et al.*, 2020). The magnitude of microtopographic variation will differ among the various associated root structures, plant morphologies, and substrate compositions between ecological settings (Diamond *et al.*, 2021), but the parabolic change in microtopography exemplified in Figure 1 will likely still apply to ecosystem state transitions within these systems. In general, microtopography will be altered if biotic or abiotic conditions change making this framework widely applicable to other transitions such as fronts associated with the migration of primary consumers (Vu and Pennings, 2021), barrier island transgression over back-barrier marshes (FitzGerald *et al.*, 2018), and warming driven vegetation shifts (i.e. shrubification (Mekonnen *et al.*, 2021) and mangrove encroachment into marshes (Osland *et al.*, 2017)). While microtopographic heterogeneity is a seldom used tool to predict or assess vulnerability, it can serve as an ecosystem vulnerability metric that directly reflects key aspects of ecological theory that operate across ecosystem and transition types.

Conclusions and Implications

While traditional applications of SET data have been used to assess wetland vulnerability using a single vertical response parameter of central tendency (e.g., average; van Wijnen and Bakker, 2001; Cahoon *et al.*, 2002, 2006; Kirwan and Temmerman, 2009; Cahoon and Guntenspergen, 2010; Cahoon, 2015), marsh vulnerability should not be determined by a single indicator (Kirwan *et al.*, 2016; Ganju *et al.*, 2017; Wasson *et al.*, 2019). More recent vulnerability indexes synthesize multiple vertical and horizontal stability metrics into a holistic assessment (Raposa *et al.*, 2016; Defne *et al.*, 2020; Ganju *et al.*, 2022); however the spatial scale of these assessments homogenize the marsh surface at the microtopographic scale. Our results indicate a correlation between increasing microtopographic variation and a traditional wetland vulnerability metric (Fig. 6), suggesting that metrics of microtopography may serve as early indicators of marsh degradation. These novel metrics could be applied to the catalog of existing SET data records, which includes globally dispersed datasets that extend up to 30 years into the past (Blum *et al.*, 2021; Saintilan *et al.*, 2022). This application could reveal if changing microtopographic variability can be used as an early indicator of degradation generally. These novel metrics in conjunction with traditional vulnerability metrics that emphasize vertical change can facilitate a holistic assessment of current and predicted marsh vulnerability. Early detection of marsh vulnerability to SLR is critical to predict imminent ecosystem state change and to take management measures before irreversible degradation of these valuable coastal ecosystems occurs.

References

Baustian, J. J., Mendelssohn, I. A., & Hester, M. W. (2012). Vegetation's importance in regulating surface elevation in a coastal salt marsh facing elevated rates of sea level rise. *Global Change Biology*, *18*, 3377–3382. https://doi.org/10.1111/j.1365-2486.2012.02792.x

Bertness, M. D., Gough, L., & Shumway, S. W. (1992). Salt tolerances and the distribution of fugitive salt marsh plants. *Ecology*, *73*, 1842–1851. https://doi.org/10.2307/1940035

Blum, L. K., Christian, R. R., Cahoon, D. R., & Wiberg, P. L. (2021). Processes influencing marsh elevation change in low- and high-elevation zones of a temperate salt marsh. *Estuaries and Coasts*, *44*, 818–833. https://doi.org/10.1007/s12237-020-00796-z

Cahoon, D. R. (2015). Estimating relative sea-level rise and submergence potential at a coastal wetland. *Estuaries and Coasts*, *38*, 1077–1084. https://doi.org/10.1007/s12237-014-9872-8

Cahoon, D. R., & Guntenspergen, G. R. (2010). Climate change, sea-level rise, and coastal wetlands. *National Wetland Newsletter*. *32*.

Cahoon, D. R., Hensel, P. F., Spencer, T., Reed, D. J., McKee, K. L., & Saintilan, N. (2006). Coastal wetland vulnerability to relative sea-level rise: wetland elevation trends and process controls. In J. T. A. Verhoeven, B. Beltman, R. Bobbink, & D. F. Whigham (Eds.), *Wetlands and Natural Resource Management* (pp. 271–292). Springer. https://doi.org/10.1007/978-3-540-33187-2_12

Cahoon, D. R., Lynch, J. C., Perez, B. C., Segura, B., Holland, R. D., Stelly, C., Stephenson, G., & Hensel, P. (2002). High-precision measurements of wetland sediment elevation: II. the rod surface elevation table. *Journal of Sedimentary Research*, *72*, 734–739. https://doi.org/10.1306/020702720734

Cahoon, D. R., Reed, D. J., & Day, J. W. (1995). Estimating shallow subsidence in microtidal salt marshes of the southeastern United States: Kaye and Barghoorn revisited. *Marine Geology*, *128*, 1–9. https://doi.org/10.1016/0025-3227(95)00087-F

Callaway, J. C., Cahoon, D. R., & Lynch, J. C. (2013). The Surface Elevation Table–Marker Horizon Method for Measuring Wetland Accretion and Elevation Dynamics. In *Methods in Biogeochemistry of Wetlands* (pp. 901–917). John Wiley & Sons, Ltd. https://doi.org/10.2136/sssabookser10.c46

Craft, C., Clough, J., Ehman, J., Joye, S., Park, R., Pennings, S., Guo, H., & Machmuller, M. (2009). Forecasting the effects of accelerated sea-level rise on tidal marsh ecosystem services. *Frontiers in Ecology and the Environment*, *7*(2), 73–78. https://doi.org/10.1890/070219

Dakos, V., Scheffer, M., van Nes, E. H., Brovkin, V., Petoukhov, V., & Held, H. (2008). Slowing down as an early warning signal for abrupt climate change. *Proceedings of the National Academy of Sciences*, *105*(38), 14308–14312. https://doi.org/10.1073/pnas.0802430105

Defne, Z., Aretxabaleta, A. L., Ganju, N. K., Kalra, T. S., Jones, D. K., & Smith, K. E. L. (2020). A geospatially resolved wetland vulnerability index: Synthesis of physical drivers. *PLOS ONE*, *15*(1), e0228504. https://doi.org/10.1371/journal.pone.0228504

DeLaune, R. D., Nyman, J. A., & Jr., W. H. P. (1994). Peat Collapse, Ponding and Wetland Loss in a Rapidly Submerging Coastal Marsh. *Journal of Coastal Research*, *10*(4), 1021–1030.

Diamond, J. S., Epstein, J. M., Cohen, M. J., McLaughlin, D. L., Hsueh, Y.-H., Keim, R. F., & Duberstein, J. A. (2021). A little relief: Ecological functions and autogenesis of wetland microtopography. *WIREs Water*, *8*(1), e1493. https://doi.org/10.1002/wat2.1493

Doughty, C. L., Ambrose, R. F., Okin, G. S., & Cavanaugh, K. C. (2021). Characterizing spatial variability in coastal wetland biomass across multiple scales using UAV and satellite imagery. *Remote Sensing in Ecology and Conservation*, *7*(3), 411–429. https://doi.org/10.1002/rse2.198

Duran Vinent, O., Herbert, E. R., Coleman, D. J., Himmelstein, J. D., & Kirwan, M. L. (2021). Onset of runaway fragmentation of salt marshes. *One Earth*, *4*(4), 506–516. https://doi.org/10.1016/j.oneear.2021.02.013

Fagherazzi, S., Kirwan, M. L., Mudd, S. M., Guntenspergen, G. R., Temmerman, S., D'Alpaos, A., van de Koppel, J., Rybczyk, J. M., Reyes, E., Craft, C., & Clough, J. (2012). Numerical models of salt marsh evolution: Ecological, geomorphic, and climatic factors. *Reviews of Geophysics*, *50*(1). https://doi.org/10.1029/2011RG000359

Farron, S. J., Hughes, Z. J., & FitzGerald, D. M. (2020). Assessing the response of the Great Marsh to sea-level rise: Migration, submersion or survival. *Marine Geology*, *425*, 106195. https://doi.org/10.1016/j.margeo.2020.106195

FitzGerald, D. M., J. Hein, C., Hughes, Z., Kulp, M., Georgiou, I., & Miner, M. (2018). Runaway Barrier Island Transgression Concept: Global Case Studies. In L. J. Moore & A. B. Murray (Eds.), *Barrier Dynamics and Response to Changing Climate* (pp. 3–56). Springer International Publishing. https://doi.org/10.1007/978-3-319-68086-6_1

Ganju, N. K., Couvillion, B. R., Defne, Z., & Ackerman, K. V. (2022). Development and Application of Landsat-Based Wetland Vegetation Cover and UnVegetated-Vegetated Marsh Ratio (UVVR) for the Conterminous United States. *Estuaries and Coasts*, *45*(7), 1861–1878. https://doi.org/10.1007/s12237-022-01081-x

Ganju, N. K., Defne, Z., Kirwan, M. L., Fagherazzi, S., D'Alpaos, A., & Carniello, L. (2017). Spatially integrative metrics reveal hidden vulnerability of microtidal salt marshes. *Nature Communications*, *8*(1), Article 1. https://doi.org/10.1038/ncomms14156

Ganju, N. K., Nidzieko, N. J., & Kirwan, M. L. (2013). Inferring tidal wetland stability from channel sediment fluxes: Observations and a conceptual model. *Journal of Geophysical Research: Earth Surface*, *118*(4), 2045–2058. https://doi.org/10.1002/jgrf.20143

Harman, C. J., Lohse, K. A., Troch, P. A., & Sivapalan, M. (2014). Spatial patterns of vegetation, soils, and microtopography from terrestrial laser scanning on two semiarid hillslopes of contrasting lithology. *Journal of Geophysical Research: Biogeosciences*, *119*(2), 163–180. https://doi.org/10.1002/2013JG002507

Harris, L. I., Roulet, N. T., & Moore, T. R. (2020). Mechanisms for the development of microform patterns in peatlands of the Hudson Bay lowland. *Ecosystems*, *23*, 741–767. https://doi.org/10.1007/s10021-019-00436-z

Himmelstein, J., Vinent, O. D., Temmerman, S., & Kirwan, M. L. (2021). Mechanisms of pond expansion in a rapidly submerging marsh. *Frontiers in Marine Science*, *8*. https://www.frontiersin.org/articles/10.3389/fmars.2021.704768

Hladik, C., & Alber, M. (2012). Accuracy assessment and correction of a LIDAR-derived salt marsh digital elevation model. *Remote Sensing of Environment*, *121*, 224–235. https://doi.org/10.1016/j.rse.2012.01.018

Hopkinson, C. S., Cai, W.-J., & Hu, X. (2012). Carbon sequestration in wetland dominated coastal systems—A global sink of rapidly diminishing magnitude. *Current Opinion in Environmental Sustainability*, *4*, 186–194. https://doi.org/10.1016/j.cosust.2012.03.005

Jankowski, K. L., Törnqvist, T. E., & Fernandes, A. M. (2017). Vulnerability of Louisiana's coastal wetlands to present-day rates of relative sea-level rise. *Nature Communications*, *8*, Article 1. https://doi.org/10.1038/ncomms14792

Kamphorst, E. C., Jetten, V., Guérif, J., Pitk a ¨ nen, J., Iversen, B. V., Douglas, J. T., & Paz, A. (2000). Predicting depressional storage from soil surface roughness. *Soil Science Society of America Journal*, *64*, 1749–1758. https://doi.org/10.2136/sssaj2000.6451749x

Karstens, S., Jurasinski, G., Glatzel, S., & Buczko, U. (2016). Dynamics of surface elevation and microtopography in different zones of a coastal Phragmites wetland. *Ecological Engineering*, *94*, 152–163. https://doi.org/10.1016/j.ecoleng.2016.05.049

Kirwan, M. L., & Megonigal, J. P. (2013). Tidal wetland stability in the face of human impacts and sea-level rise. *Nature*, *504*, Article 7478. https://doi.org/10.1038/nature12856

Kirwan, M. L., Temmerman, S., Skeehan, E. E., Guntenspergen, G. R., & Fagherazzi, S. (2016). Overestimation of marsh vulnerability to sea level rise. *Nature Climate Change*, *6*, Article 3. https://doi.org/10.1038/nclimate2909

Kirwan, M., & Temmerman, S. (2009). Coastal marsh response to historical and future sea-level acceleration. *Quaternary Science Reviews*, *28*, 1801–1808. https://doi.org/10.1016/j.quascirev.2009.02.022

Langston, A. K., Alexander, C. R., Alber, M., & Kirwan, M. L. (2021). Beyond 2100: Elevation capital disguises salt marsh vulnerability to sea-level rise in Georgia, USA. *Estuarine, Coastal and Shelf Science*, *249*, 107093. https://doi.org/10.1016/j.ecss.2020.107093

Langston, A. K., Durán Vinent, O., Herbert, E. R., & Kirwan, M. L. (2020). Modeling long-term salt marsh response to sea level rise in the sediment-deficient Plum Island Estuary, MA. *Limnology and Oceanography*, *65*, 2142–2157. https://doi.org/10.1002/lno.11444

Lovelock, C. E., Cahoon, D. R., Friess, D. A., Guntenspergen, G. R., Krauss, K. W., Reef, R., Rogers, K., Saunders, M. L., Sidik, F., Swales, A., Saintilan, N., Thuyen, L. X., & Triet, T. (2015). The vulnerability of Indo-Pacific mangrove forests to sea-level rise. *Nature*, *526*, Article 7574. https://doi.org/10.1038/nature15538

Lynch, J., Hensel, P., & Cahoon, D. (2015). The surface elevation table and marker horizon technique: a protocol for monitoring wetland elevation dynamics. *(No. NPS/NCBN/NRR—2015/1078). National Park Service.*

Marion, C., Anthony, E. J., & Trentesaux, A. (2009). Short-term (≤2 yrs) estuarine mudflat and saltmarsh sedimentation: High-resolution data from ultrasonic altimetery, rod surface-elevation table, and filter traps. *Estuarine, Coastal and Shelf Science*, *83*, 475–484. https://doi.org/10.1016/j.ecss.2009.03.039

Mariotti, G. (2016). Revisiting salt marsh resilience to sea level rise: Are ponds responsible for permanent land loss?: *Journal of Geophysical Research: Earth Surface*, *121*, 1391–1407. https://doi.org/10.1002/2016JF003900

Mariotti, G. (2020). Beyond marsh drowning: The many faces of marsh loss (and gain). *Advances in Water Resources*, *144*, 103710. https://doi.org/10.1016/j.advwatres.2020.103710

Mariotti, G., & Carr, J. (2014). Dual role of salt marsh retreat: Long-term loss and short-term resilience. *Water Resources Research*, *50*, 2963–2974. https://doi.org/10.1002/2013WR014676

Mariotti, G., & Fagherazzi, S. (2013). Critical width of tidal flats triggers marsh collapse in the absence of sea-level rise. *Proceedings of the National Academy of Sciences*, *110*, 5353–5356. https://doi.org/10.1073/pnas.1219600110

Mariotti, G., Spivak, A. C., Luk, S. Y., Ceccherini, G., Tyrrell, M., & Gonneea, M. E. (2020). Modeling the spatial dynamics of marsh ponds in New England salt marshes. *Geomorphology*, *365*, 107262. https://doi.org/10.1016/j.geomorph.2020.107262

McClure, A., Liu, X., Hines, E., & Ferner, M. C. (2015). Evaluation of error reduction techniques on a lidar-derived salt marsh digital elevation model. *Journal of Coastal Research*, *32*, 424–433. https://doi.org/10.2112/JCOASTRES-D-14-00185.1

Mekonnen, Z. A., Riley, W. J., Berner, L. T., Bouskill, N. J., Torn, M. S., Iwahana, G., Breen, A. L., Myers-Smith, I. H., Criado, M. G., Liu, Y., Euskirchen, E. S., Goetz, S. J., Mack, M. C., & Grant, R. F. (2021). Arctic tundra shrubification: A review of mechanisms and impacts on ecosystem carbon balance. *Environmental Research Letters*, *16*, 053001. https://doi.org/10.1088/1748-9326/abf28b

Moser, K., Ahn, C., & Noe, G. (2007). Characterization of microtopography and its influence on vegetation patterns in created wetlands. *Wetlands*, *27*, 1081–1097. https://doi.org/10.1672/0277-5212(2007)27[1081:COMAII]2.0.CO;2

Neijnens, F. K., Siteur, K., van de Koppel, J., & Rietkerk, M. (2021). Early warning signals for rate-induced critical transitions in salt marsh ecosystems. *Ecosystems*, *24*, 1825–1836. https://doi.org/10.1007/s10021-021-00610-2

Osland, M. J., Feher, L. C., Griffith, K. T., Cavanaugh, K. C., Enwright, N. M., Day, R. H., Stagg, C. L., Krauss, K. W., Howard, R. J., Grace, J. B., & Rogers, K. (2017). Climatic controls on the global distribution, abundance, and species richness of mangrove forests. *Ecological Monographs*, *87*, 341–359. https://doi.org/10.1002/ecm.1248

Raposa, K. B., Wasson, K., Smith, E., Crooks, J. A., Delgado, P., Fernald, S. H., Ferner, M. C., Helms, A., Hice, L. A., Mora, J. W., Puckett, B., Sanger, D., Shull, S., Spurrier, L., Stevens, R., & Lerberg, S. (2016). Assessing tidal marsh resilience to sea-level rise at broad geographic scales with multi-metric indices. *Biological Conservation*, *204*, 263–275. https://doi.org/10.1016/j.biocon.2016.10.015

Reed, D. J. (1995). The response of coastal marshes to sea-level rise: Survival or submergence? *Earth Surface Processes and Landforms*, *20*, 39–48. https://doi.org/10.1002/esp.3290200105

Saintilan, N., Kovalenko, K. E., Guntenspergen, G., Rogers, K., Lynch, J. C., Cahoon, D. R., Lovelock, C. E., Friess, D. A., Ashe, E., Krauss, K. W., Cormier, N., Spencer, T., Adams, J., Raw, J., Ibanez, C., Scarton, F., Temmerman, S., Meire, P., Maris, T., … Khan, N. (2022). Constraints on the adjustment of tidal marshes to accelerating sea level rise. *Science*, *377*, 523–527. https://doi.org/10.1126/science.abo7872

Scheffer, M., Carpenter, S., Foley, J. A., Folke, C., & Walker, B. (2001). Catastrophic shifts in ecosystems. *Nature*, *413*, Article 6856. https://doi.org/10.1038/35098000

Schepers, L., Brennand, P., Kirwan, M. L., Guntenspergen, G. R., & Temmerman, S. (2020). Coastal marsh degradation into ponds induces irreversible elevation loss relative to sea level in a microtidal system. *Geophysical Research Letters*, *47*, e2020GL089121. https://doi.org/10.1029/2020GL089121

Schepers, L., Kirwan, M. L., Guntenspergen, G. R., & Temmerman, S. (2020). Evaluating indicators of marsh vulnerability to sea level rise along a historical marsh loss gradient. *Earth Surface Processes and Landforms*, *45*, 2107–2117. https://doi.org/10.1002/esp.4869

Smith, A. J., Noyce, G. L., Megonigal, J. P., Guntenspergen, G. R., & Kirwan, M. L. (2022). Temperature optimum for marsh resilience and carbon accumulation revealed in a whole-ecosystem warming experiment. *Global Change Biology*, *28*, 3236–3245. https://doi.org/10.1111/gcb.16149

Steinmuller, H. E., Bourque, E., Lucas, S. B., Engelbert, K. M., Garwood, J., & Breithaupt, J. L. (2022). Comparing Vertical Change in Riverine, Bayside, and Barrier Island Wetland Soils in Response to Acute and Chronic Disturbance in Apalachicola Bay, FL. *Estuaries and Coasts*. https://doi.org/10.1007/s12237-022-01131-4

Stevenson, J. C., Kearney, M. S., & Pendleton, E. C. (1985). Sedimentation and erosion in a Chesapeake Bay brackish marsh system. *Marine Geology*, *67*(3), 213–235. https://doi.org/10.1016/0025-3227(85)90093-3

Stribling, J. M., Cornwell, J. C., & Glahn, O. A. (2007). Microtopography in tidal marshes: Ecosystem engineering by vegetation? *Estuaries and Coasts*, *30*, 1007–1015. https://doi.org/10.1007/BF02841391

Temmerman, S., Meire, P., Bouma, T. J., Herman, P. M. J., Ysebaert, T., & De Vriend, H. J. (2013). Ecosystem-based coastal defence in the face of global change. *Nature*, *504*, Article 7478. https://doi.org/10.1038/nature12859

Törnqvist, T. E., Cahoon, D. R., Morris, J. T., & Day, J. W. (2021). Coastal wetland resilience, accelerated sea-level rise, and the importance of timescale. *AGU Advances*, *2*, e2020AV000334. https://doi.org/10.1029/2020AV000334

van Belzen, J., van de Koppel, J., Kirwan, M. L., van der Wal, D., Herman, P. M. J., Dakos, V., Kéfi, S., Scheffer, M., Guntenspergen, G. R., & Bouma, T. J. (2017). Vegetation recovery in tidal marshes reveals critical slowing down under increased inundation. *Nature Communications*, *8*, Article 1. https://doi.org/10.1038/ncomms15811

van Nes, E. H., & Scheffer, M. (2007). Slow recovery from perturbations as a generic indicator of a nearby catastrophic shift. *The American Naturalist*, *169*(6), 738–747. https://doi.org/10.1086/516845

van Wijnen, H. J., & Bakker, J. P. (2001). Long-term surface elevation change in salt marshes: a prediction of marsh response to future sea-level rise. *Estuarine, Coastal and Shelf Science*, *52*, 381–390. https://doi.org/10.1006/ecss.2000.0744

Vu, H. D., & Pennings, S. C. (2021). Directional movement of consumer fronts associated with creek heads in salt marshes. *Ecology*, *102*, e03447. https://doi.org/10.1002/ecy.3447

Wang, C., Schepers, L., Kirwan, M. L., Belluco, E., D'Alpaos, A., Wang, Q., Yin, S., & Temmerman, S. (2021). Different coastal marsh sites reflect similar topographic conditions under which bare patches and vegetation recovery occur. *Earth Surface Dynamics*, *9*, 71–88. https://doi.org/10.5194/esurf-9-71-2021

Wang, C., & Temmerman, S. (2013). Does biogeomorphic feedback lead to abrupt shifts between alternative landscape states?: An empirical study on intertidal flats and marshes. *Journal of Geophysical Research: Earth Surface*, *118*, 229–240. https://doi.org/10.1029/2012JF002474

Wasson, K., Ganju, N. K., Defne, Z., Endris, C., Elsey-Quirk, T., Thorne, K. M., Freeman, C. M., Guntenspergen, G., Nowacki, D. J., & Raposa, K. B. (2019). Understanding tidal marsh trajectories: Evaluation of multiple indicators of marsh persistence. *Environmental Research Letters*, *14*, 124073. https://doi.org/10.1088/1748-9326/ab5a94

Watson, E. B., Wigand, C., Davey, E. W., Andrews, H. M., Bishop, J., & Raposa, K. B. (2017). Wetland loss patterns and inundation-productivity relationships prognosticate widespread salt marsh loss for Southern New England. *Estuaries and Coasts*, *40*, 662–681. https://doi.org/10.1007/s12237-016-0069-1

Webb, E. L., Friess, D. A., Krauss, K. W., Cahoon, D. R., Guntenspergen, G. R., & Phelps, J. (2013). A global standard for monitoring coastal wetland vulnerability to accelerated sea-level rise. *Nature Climate Change*, *3*, Article 5. https://doi.org/10.1038/nclimate1756

Werner, K. J., & Zedler, J. B. (2002). How sedge meadow soils, microtopography, and vegetation respond to Sedimentation. *Wetlands*, *22*, 451–466. https://doi.org/10.1672/0277-5212(2002)022[0451:HSMSMA]2.0.CO;2

Wilson, C. A., Hughes, Z. J., FitzGerald, D. M., Hopkinson, C. S., Valentine, V., & Kolker, A. S. (2014). Saltmarsh pool and tidal creek morphodynamics: Dynamic equilibrium of northern latitude saltmarshes? *Geomorphology*, *213*, 99–115. https://doi.org/10.1016/j.geomorph.2014.01.002

Wilson, J. B., & Agnew, A. D. Q. (1992). Positive-feedback Switches in Plant Communities. In M. Begon & A. H. Fitter (Eds.), *Advances in Ecological Research* (Vol. 23, pp. 263–336). Academic Press. https://doi.org/10.1016/S0065-2504(08)60149-X

Yeates, A. G., Grace, J. B., Olker, J. H., Guntenspergen, G. R., Cahoon, D. R., Adamowicz, S., Anisfeld, S. C., Barrett, N., Benzecry, A., Blum, L., Christian, R. R., Grzyb, J., Hartig, E. K., Leo, K. H., Lerberg, S., Lynch, J. C., Maher, N., Megonigal, J. P., Reay, W., and Warren, S. (2020). Hurricane Sandy effects on coastal marsh elevation change. *Estuaries and Coasts*, *43*, 1640–1657. https://doi.org/10.1007/s12237-020-00758-5

Tables and Figures

Table 1. Environmental characteristics at the site and SET level for eight tidal salt marshes along the Atlantic Coast of the United States. Every SET is accompanied with elevation data of the marsh surface in m in NAVD88 and D, the dimensionless position within the tidal frame where positive values indicate an elevation greater than mean high water (calculated from mean high water minus elevation divided by the tidal range (Morris, 2006; Kefelegn, 2019)), and the dominant vegetation surrounding the plot at the point of installation. Site level characteristics include regional 50-year averaged rates of SLR (sea-level rise, mm y^{-1}) (NOAA Sea Level Trends, 2023), porewater salinity (ppt) measured in April to May of 2006, and the ratio of unvegetated to vegetated marsh surface (UVVR) within 10 ha patches including both SETs at each site.

State	SET Label	Elevation (m, NAVD88)	D	SLR (mm y^{-1})	Salinity (ppt)	UVVR	Dominant Vegetation
VA	SX2	0.452	-0.68	4.00	17.4	0.07	S. patens
	SX4	0.379	-0.68				D. spicata
MD	FB8A2	0.487	-0.77	3.89	11.4	0.09	S. patens
	FB8A3	0.461	-0.81				S. americanus
	FB8D1	0.402	-1.09	3.89	10.8	0.09	S. patens
	FB8D4	0.413	-0.99				S. patens

	BW7A1	0.169	0.11	3.89	10.6	0.94	S. americanus
	BW7A3	0.136	0.23				S. americanus
	BW7D1	0.122	0.28	3.89	9.6	0.94	S. americanus
	BW7D4	0.123	0.27				S. alterniflora
	HI2	0.344	-0.55	3.73	8.9	0.001	S. americanus
	HI3	0.337	-0.52				S. americanus
	EN2	0.308	-0.42	3.73	11.2	0.15	S. americanus
	EN3	0.416	-0.45				S. americanus
DE	BH2	0.914	-0.03	3.76	13.6	0.16	D. spicata
	BH3	0.823	0.02				S. patens
CT	GM1	1.329	-0.18	3.14	16.0	0.42	S. americanus
	GM3	1.379	-0.2				S. americanus
ME	RC1	1.369	-0.06	1.90	19.9	0.24	D. spicata
	RC3	1.348	-0.04				G. maritima

Table 2. Marsh Vulnerability Report Card. A summary table of traditional and microtopographic vulnerability metrics for eight tidal salt marshes along the Atlantic Coast of the United States.

The calculated elevation change deficit (E_{def}, mm y^{-1}) is written out while the table depicts in red if a microtopographic metric (random roughness (RR), Tortuosity (T), elevation range (ΔH), or surface area to map area ratio (SA:MA)) detected vulnerability. SETs are grouped within their respective states and ordered latitudinally from left to right.

	VA		MD												DE		CT		ME	
	SX2	SX4	FBA2	FBA3	FBD1	FBD4	BWA1	BWA3	BWD1	BWD4	HI2	HI3	EN2	EN3	BH2	BH3	GM1	GM3	RC1	RC3
E_{def}	-0.453	-1.58	0.802	-0.201	-1.375	-11.7	1.49	1.19	-0.056	-4.83	-0.533	-0.762	-2.12	-1.78	2.19	-0.163	-0.467	-1.17	2.01	1.45
RR	■	■		■	■	■	■	■	■	■			■	■				■		
T	■	■			■	■		■		■			■					■		
ΔH	■	■		■	■	■		■		■	■	■	■					■		
SA: MA		■			■	■				■			■					■		
Total	3	4	0	2	4	4	1	3	1	4	1	1	4	1	0	0	0	4	0	0

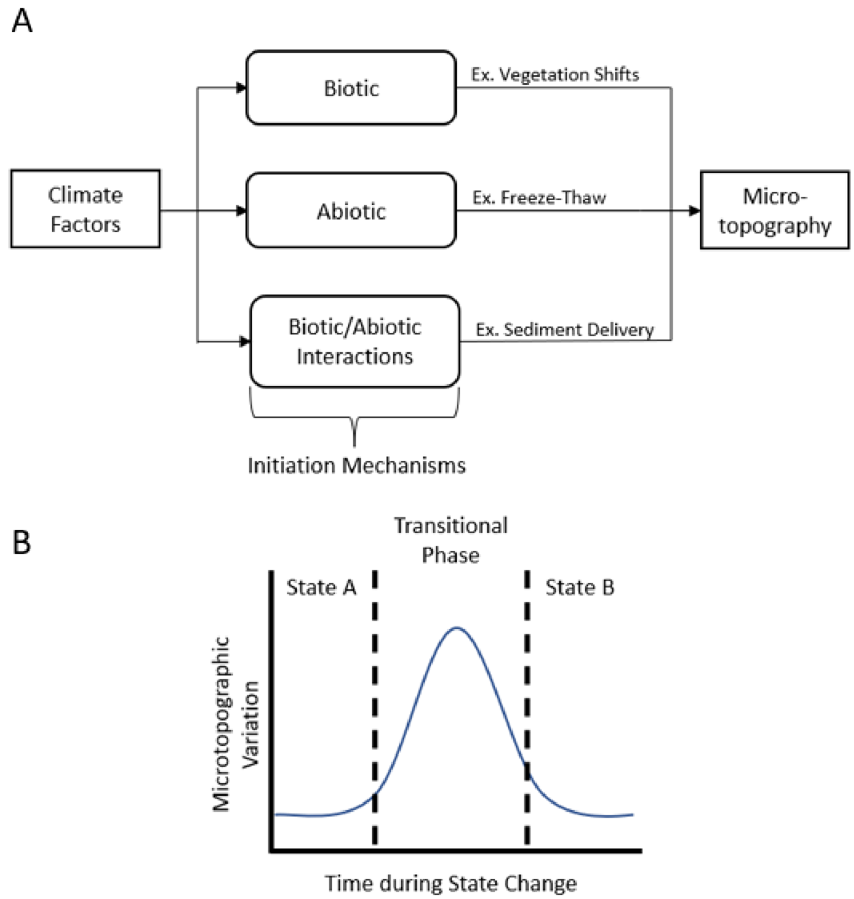

Fig. 1 (a) Conceptual diagram of the influence of climate on microtopographic initiation in wetlands (adapted from Diamond *et al.*, (2020)). Initiation mechanisms create small-scale variation in soil elevation. These mechanisms can be modulated by climate factors, such as elevated atmospheric CO_2 concentrations, warming, and enhanced productivity, that affect biotic and abiotic drivers of microtopography. (b) Conceptual diagram of increased spatial variation associated with the transition between two alternative stable states. As a stable ecosystem (State A) approaches the critical threshold of a state change, spatial variation (e.g. microtopographic variation, landscape heterogeneity, etc.) is expected to increase and is maximized during the transitional phase when the reference frame is a mosaic of either alternative states. As the

alternative state (State B) dominates the reference frame, spatial variation is expected to decrease to the state's equilibrium conditions.

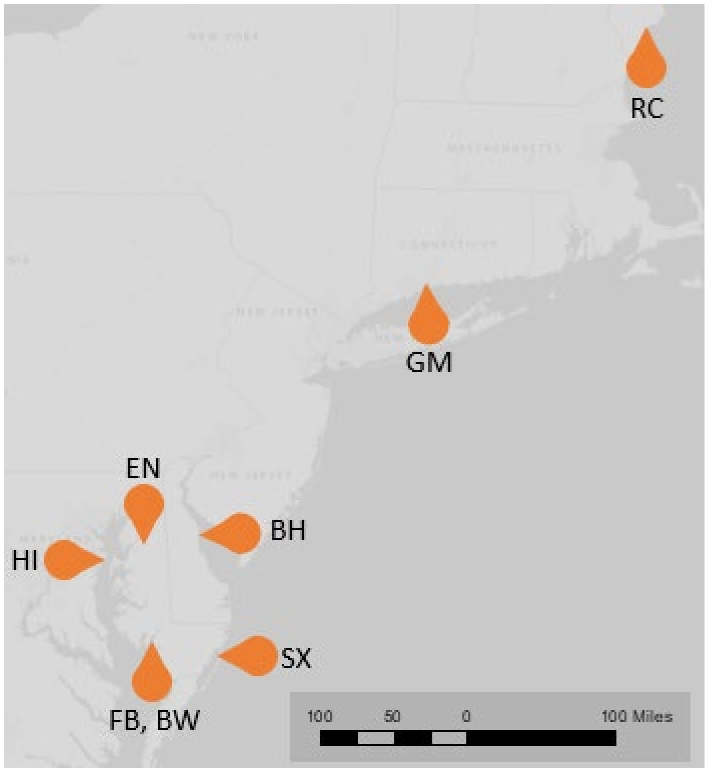

Fig. 2 A general map of the mid-Atlantic region of North America showing site names and locations. The southernmost site is in Virginia (SX, Saxis Wildlife Management Area), six sites are located in Maryland (FB, Fishing Bay Wildlife Management Area; BW, Blackwater National Wildlife Refuge; HI, Hog Island at the Smithsonian Environmental Research Center; EN, Eastern Neck National Wildlife Refuge), and one site is located in Delaware (BH, Bombay Hook National Wildlife Refuge), Connecticut (GM, Great Meadows National Wildlife Refuge), and Maine (RC, Rachel Carbon National Wildlife Refuge). Each site contains two SET stations, except for FB and BW, which contain four SET stations each.

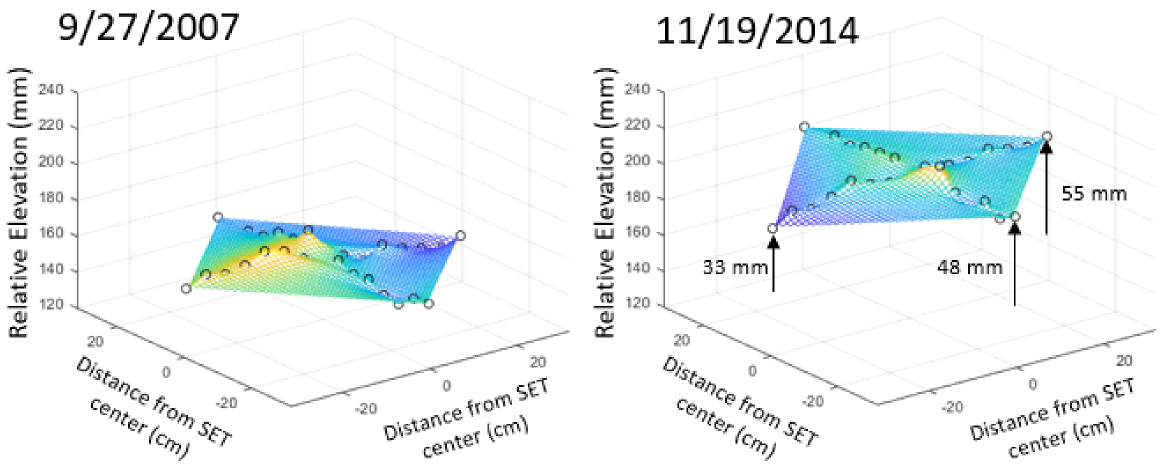

Fig. 3 Interpolated mesh-grid of the marsh surface at BH2 (Bombay Hook National Wildlife Refuge, Maryland, U.S., SET2) on September 27th, 2007 and November 19th, 2014. These interpolated surfaces were created for all SETs during all measurement collections and serve as the surface utilized in the SA:MA microtopographic variability metric. The color of the grid is relative to the height extremes of the marsh surface during each sampling period with the highest point in yellow and the lowest point in blue. The black open circles represent the SET derived measurements from the respective dates that were used to interpolate the surface. Arrows demarcate the change in elevation of identical locations in the marsh surface measured between the two time points.

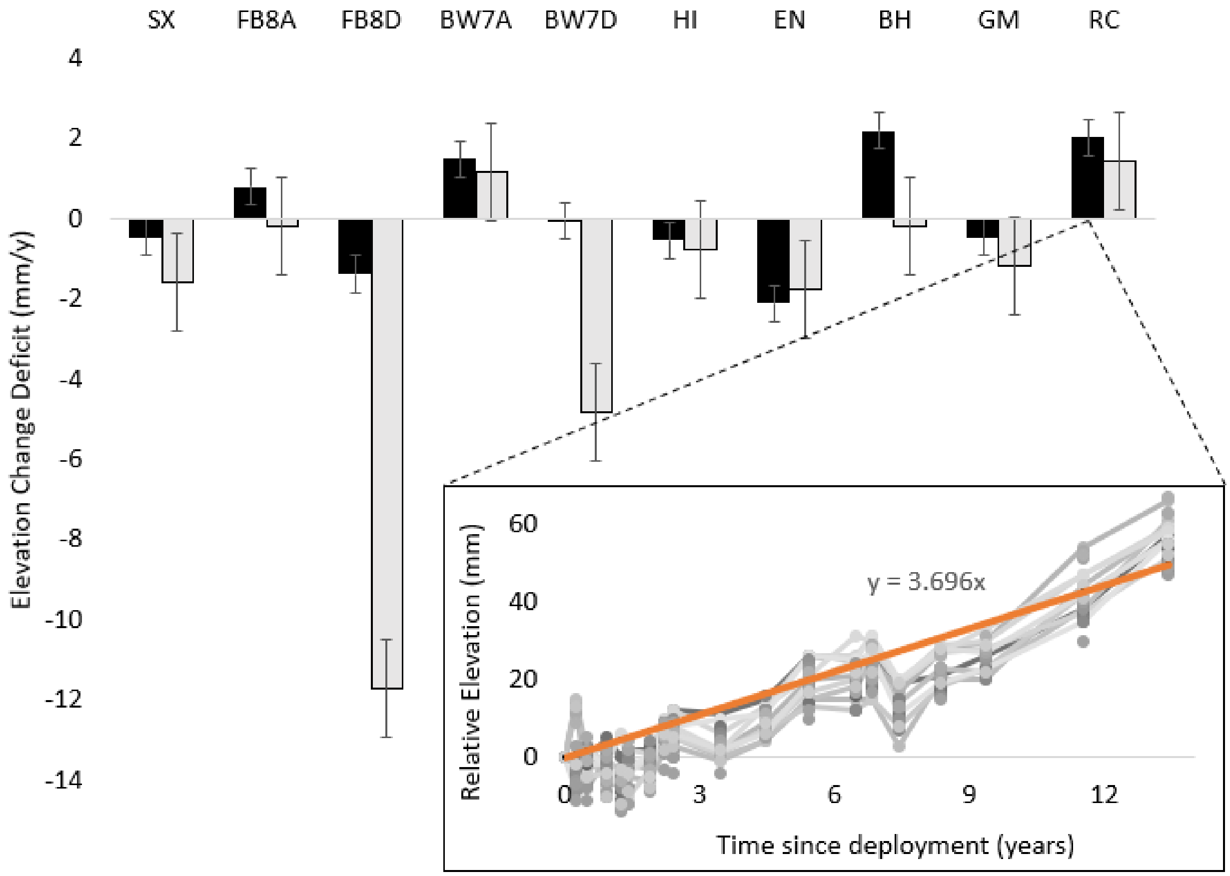

Fig. 4 The elevation change deficits (mm y^{-1}) calculated from the surface elevation tables (SETs) reviewed in this study. Positive elevation change deficits indicate that the rate of elevation change is greater than the rate of sea-level rise (SLR) while negative elevation change deficits indicate that the rate of SLR is greater than the rate of elevation change (see Methods section). SETs are grouped by site with the respective site abbreviation above the paired stations. These are then organized from left to right in order of increasing latitude. The gray and black colors of the bar differentiate the SET stations present within each site and are not representative of any treatment or applied condition. Elevation change deficit is the difference between elevation change (mm y^{-1}) and 50-year average rate of SLR (mm y^{-1}). Elevation change at each SET was determined by averaging the rate of elevation change of each individual pin (n=~30) across the

time period, exemplified by the inset of SET pin trajectories at RC1 shown in grays with the calculated average elevation change shown in orange. Error bars within the bar chart represent the standard deviation of the average elevation change deficit.

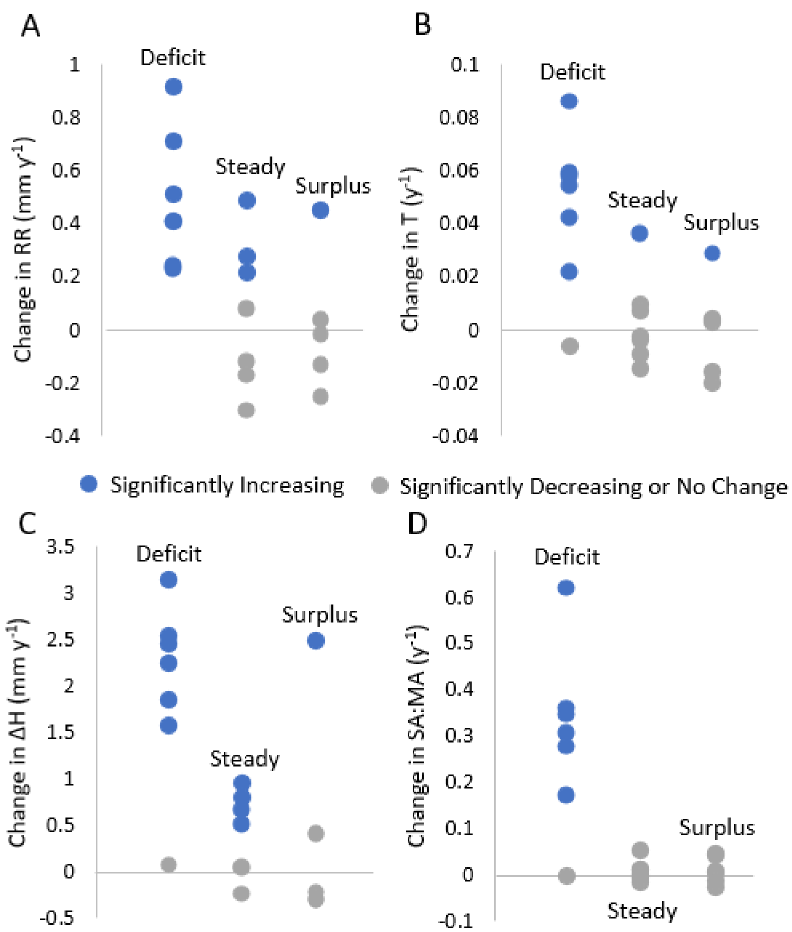

Fig. 5 Categorical scatterplots of rates of changes of the four microtopographic variability metrics, (a) random roughness (RR), (b) tortuosity (T), (c) elevation range (ΔH), (d) the surface area to map area ratio (SA:MA), grouped according to traditional metrics of vulnerability (i.e. elevation change deficits). The “Deficit” category refers to surface elevation tables (SETs) where the elevation change was less than the 50-year averaged rate of local sea-level rise (SLR), while the “steady” and “surplus” categories indicate SETs where the elevation change was not different or significantly greater than the rate of local SLR. The color of the datapoint represents whether

the linear regression calculated for the respective vulnerability metrics is either significantly increasing through time (blue) or decreasing or not significantly changing (both in gray).

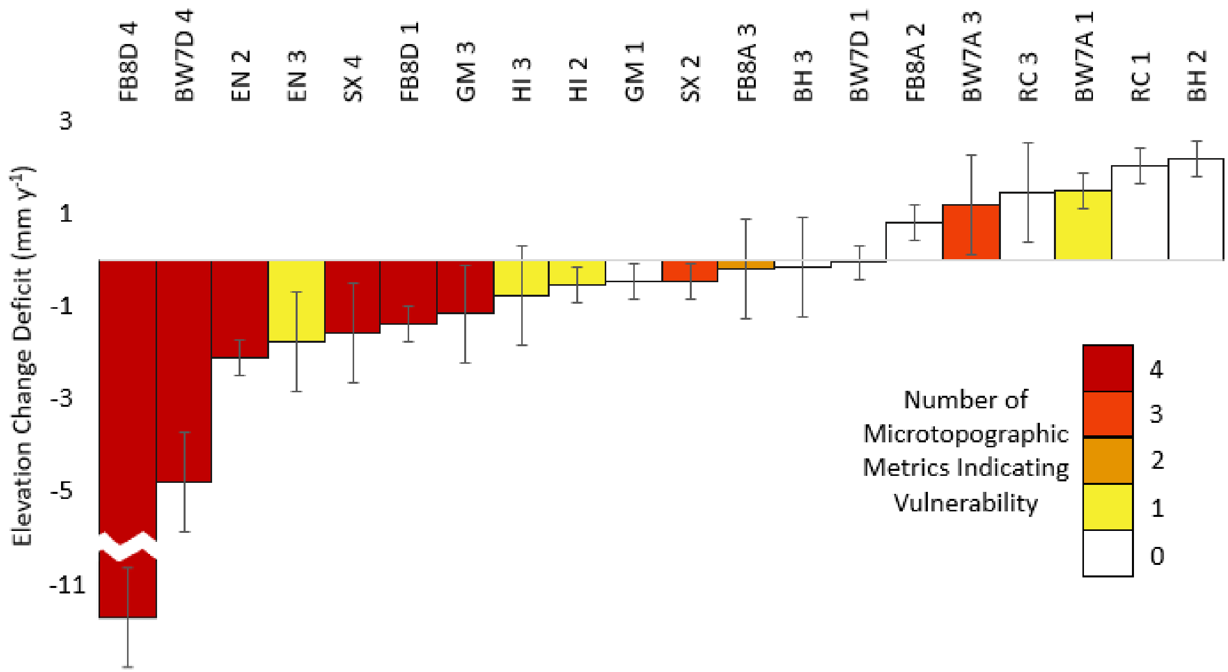

Fig. 6 Comparison of traditional vulnerability metrics (elevation change deficit) with the novel microtopographic vulnerability metrics for eight tidal salt marshes along the Atlantic Coast of the United States. Elevation change deficit data are the same data displayed in Fig. 4, but arranged from lowest to highest elevation change deficit with the respective SET label displayed above. Positive elevation change deficits indicate that the rate of elevation change is greater than the rate of SLR while negative elevation change deficits indicate that the rate of SLR is greater than the rate of elevation change (see Methods section). The color of the bars is determined by the number of microtopographic metrics that indicated vulnerability (Table 2). From this, we can see that six of the seven most vulnerable sites identified by traditional metrics are also identified as vulnerable according to every novel microtopographic vulnerability metric. Error bars represent standard error.